Electronic Supplementary Information

Experimental and theoretical insight into sustained water splitting with electrodeposited nanoporous nickel hydroxide@nickel film as a electrocatalyst

Zhicai Xing,[‡a] Linfeng Gan,[‡a] Jin Wang*[ab] and Xiurong Yang*[a]

[a]State Key Laboratory of Electroanalytical Chemistry, Changchun Institute of Applied Chemistry, Chinese Academy of Sciences, Changchun 130022, Jilin (China)
E-mail: jin.d.wang@gmail.com; xryang@ciac.ac.cn
[b]Department of Chemistry and Physics, State University of New York at Stony Brook, New York, NY 11794-3400 (USA)

Experimental Section

Materials

Carbon cloth (CC) was provided by Hongshan District, Wuhan Instrument Surgical Instruments Business. $NiSO_4 \cdot 6H_2O$, $Ni(NO_3)_2 \cdot 6H_2O$, and KOH were purchased from Aladdin Ltd. (Shanghai, China). Pt/C (20 wt% Pt on Vulcan XC-72R), Nafion (5 wt%), and $RuCl_3 \cdot xH_2O$ were purchased from Sigma-Aldrich. The water used throughout all experiments was purified through a Millipore system.

Preparation of $Ni(OH)_2$@Ni/CC

Typically, the electrodeposition process was carried out in a three-electrode cell using CC or $Ni(OH)_2$/CC as the working electrode, a graphite plate as the counter electrode, and Ag/AgCl (3 M KCl) as the reference electrode. $Ni(OH)_2$ was directly

electrodeposited on a piece of CC (1 cm × 2 cm) from 0.1 M $Ni(NO_3)_2$ aqueous solution at a constant potential of -1.0 V (vs. the saturated calomel electrode (SCE)) for 420 s at 25 °C. Then, Ni was electrodeposited on the surface of $Ni(OH)_2$/CC by performing cyclic voltammogram for 20 cycles at a sweep rat of 50 mV s^{-1} in 0.1 M $NiSO_4 \cdot 6H_2O$ aqueous solution. After deposition, the $Ni(OH)_2$@Ni/CC was removed from the cell, rinsed with deionized water for several times, and dried by nitrogen flow. The reference sample, Ni/CC was prepared through the similar method to $Ni(OH)_2$@Ni/CC using the CC as the working electrode. The loading for $Ni(OH)_2$@Ni on CC was determined to be 2.8 mg cm^{-2} with the use of a high precision microbalance.

The Ni@$Ni(OH)_2$/CC electrode was also prepared by electrodeposition of $Ni(OH)_2$ on the surface of Ni/CC substrate for the comparison purpose.

Characterizations

Powder XRD data were acquired on a RigakuD/MAX 2550 diffractometer with Cu Kα radiation (λ=1.5418 Å). SEM measurements were carried out on a XL30 ESEM FEG microscope at an accelerating voltage of 20 kV. XPS measurements were performed on an ESCALABMK II X-ray photoelectron spectrometer using Mg as the exciting source. TEM measurements were performed on a HITACHI H-8100 electron microscopy (Hitachi, Tokyo, Japan) with an accelerating voltage of 200 kV.

Electrochemical measurements

All the electrochemical measurements were conducted using a CHI660E potentiostat (CH Instruments, China) in a typical three-electrode setup, using a piece

of freshly made $Ni(OH)_2$@Ni/CC as the working electrode, a graphite rod as the counter electrode and a saturated calomel electrode (SCE) as the reference electrode. Pt/C and RuO_2 were loaded on CC (mass loading: 2.8 mg cm^{-2}) for comparison, respectively. Prior to measurement, a resistance test was made and the iR compensation was applied to all initial data for further analysis. EIS measurements were carried out in the frequency range of 100 kHz–0.1 Hz. In all measurements, the SCE reference electrode was calibrated with respect to RHE. In 1.0 M KOH, E (RHE) = E (SCE) + 1.067 V. LSV curves were conducted in electrolyte with scan rate of 5 mV s^{-1} without any activation. The long-term durability test was performed using chronopotentiometric measurements. All the potentials reported in our work were expressed vs. the RHE.

Computational Section

All calculations were performed in this study using density functional theory (DFT) with the program package of DMol3[S1,S2] in the Materials Studio of BIOVIA Inc. The exchange-correlation energy was described by local functionals (LDA) using the PWC[S3] function. All electron relativistic and polarization double numerical basis-set (DNP) was employed to all elements. DFT simulations were performed based on the experimentally crystal structure[S4] of $Ni(OH)_2$ (ICSD collection code: 109391). A charge density mixing of 0.01 was used to all calculations. Previous surface morphology study[S5] showed that the 110 is one favor surface, which was further used for investigating $Ni(OH)_2$ active surface. Chemisorption surfaces were constructed as slab consists of eight layers in 3 × 3 super cells, which separated by 20

Å vacuum. The Monkhorst-Pack[S6] sampling scheme with 5 × 3 × 3 was used for $Ni(OH)_2$ geometrical optimization. And a 3 × 3 × 1 sampling scheme was used to calculate all the interaction energies. All calculations were performed with spin-polarization.

It is important to make sure that the surfaces structures we create are stable enough for catalyzing HER reaction, and thus the study of surface energy is necessary. The formula used for calculating surface energy is as below:

$$\gamma_{surf} = \frac{1}{2A_0}\left(E_{slab} - \sum_i N_i \mu_i\right)$$

Where, γ_{surf} is the surface energy, E_{slab} is the total surface slab energy, N_i is the numbers of the corresponding atoms in the surface, μ_i is the chemical potentials of the corresponding type of atoms.

Previous studies showed that the hydrogen evolution activity is strongly correlated with the free energy of hydrogen to the electrocatalyst surface.[S7,S8] The free energy change for H* adsorption on Ni, $Ni(OH)_2$ and $Ni(OH)_2$@Ni surfaces (ΔG_H) was calculated as follows, which is proposed by Norskov and coworkers[S9]:

$$\Delta G_H = E_{total} - E_{sur} - E_{H2}/2 + \Delta E_{ZPE} - T\Delta S$$

where E_{total} is the total energy for the adsorption state, E_{sur} is the energy of pure surface, E_{H2} is the energy of H_2 in gas phase, ΔE_{ZPE} is the zero-point energy change and ΔS is the entropy change.

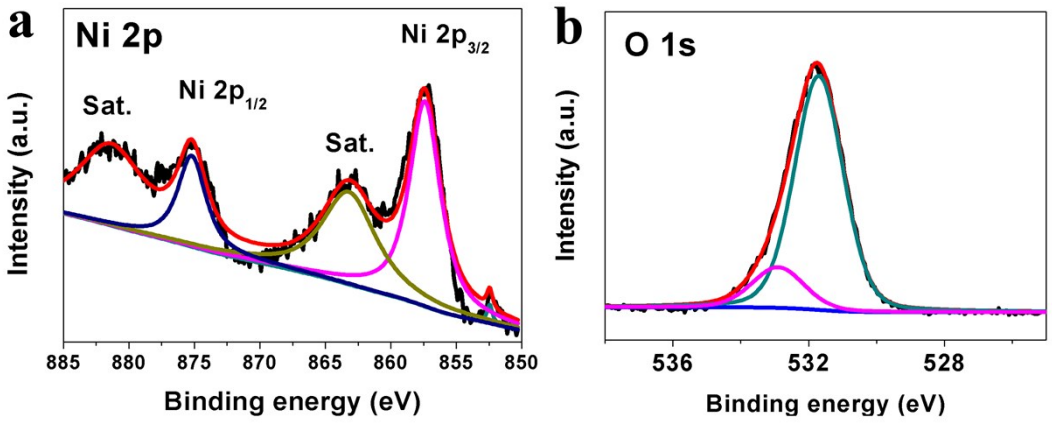

Fig. S1 XPS spectra in the (a) Ni 2p and (b) O 1s regions for $Ni(OH)_2$@Ni/CC.

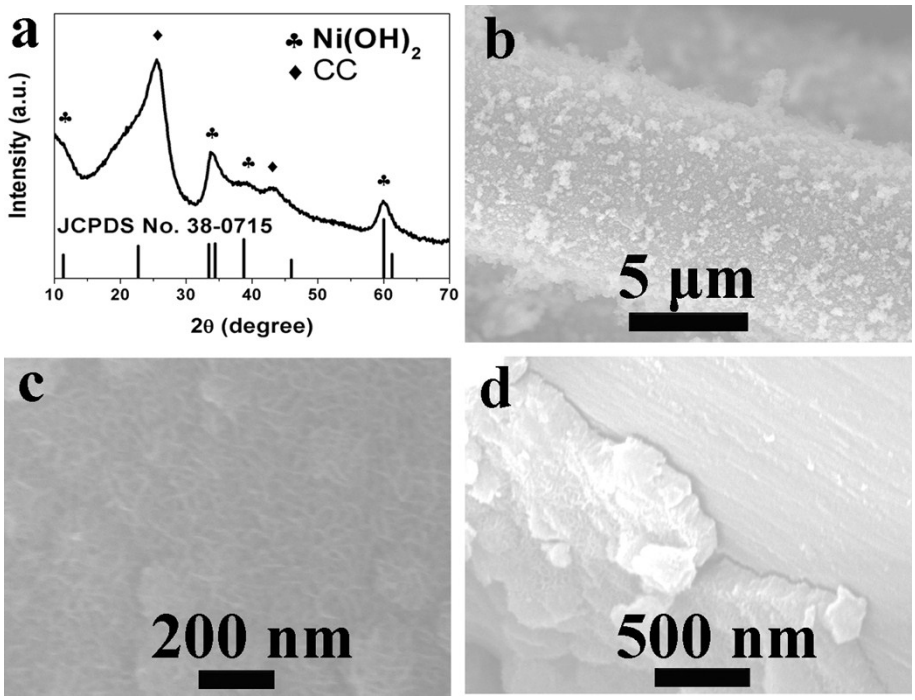

Fig. S2 (a) XRD pattern and (b, c, d) SEM images of $Ni(OH)_2$/CC.

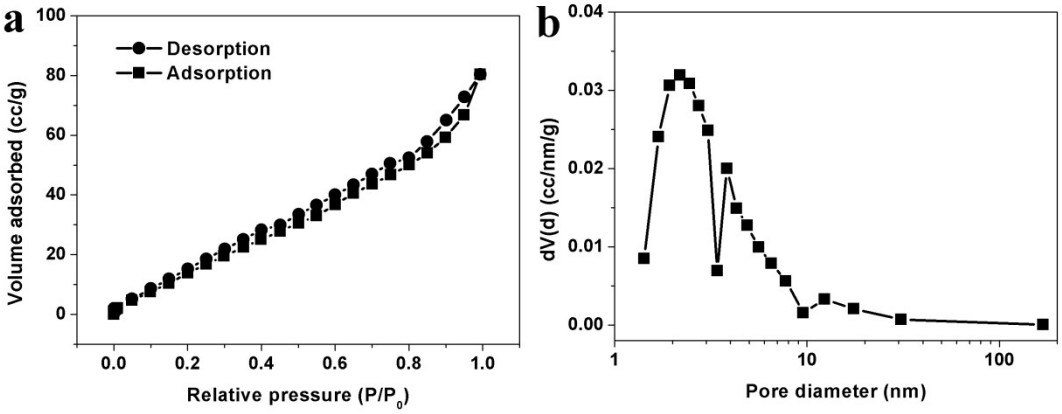

Fig. S3 (a) N_2 adsorption-desorption isotherm and (b) pore size distribution of $Ni(OH)_2$@Ni/CC.

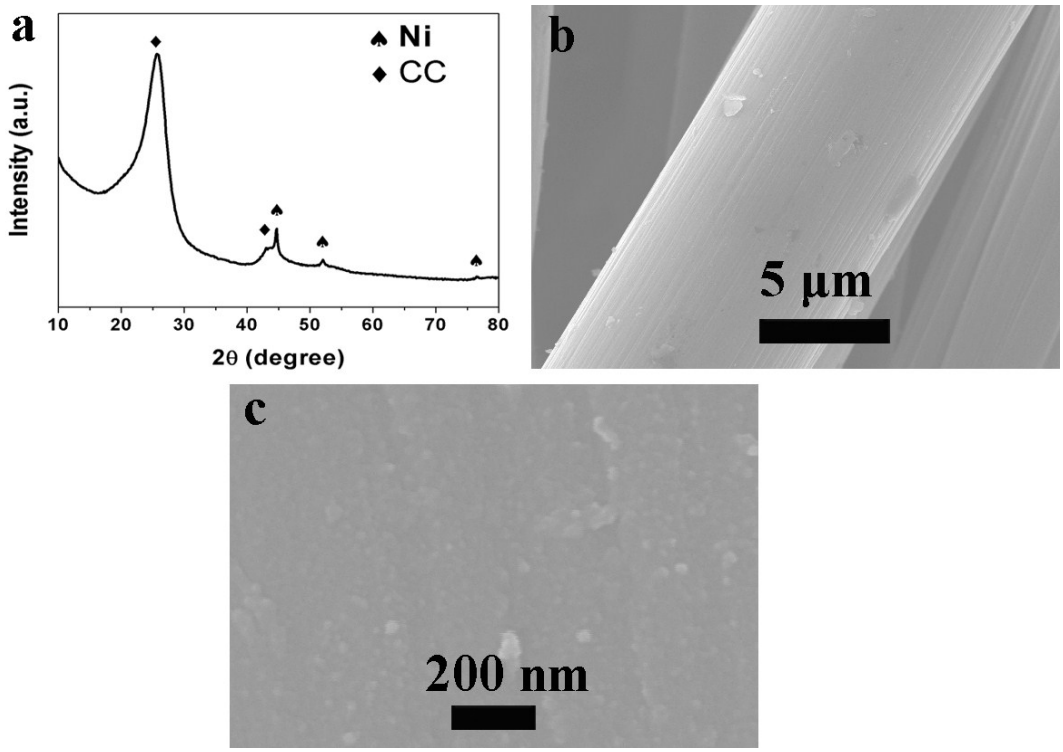

Fig. S4 (a) XRD pattern and (b, c) SEM images of Ni/CC.

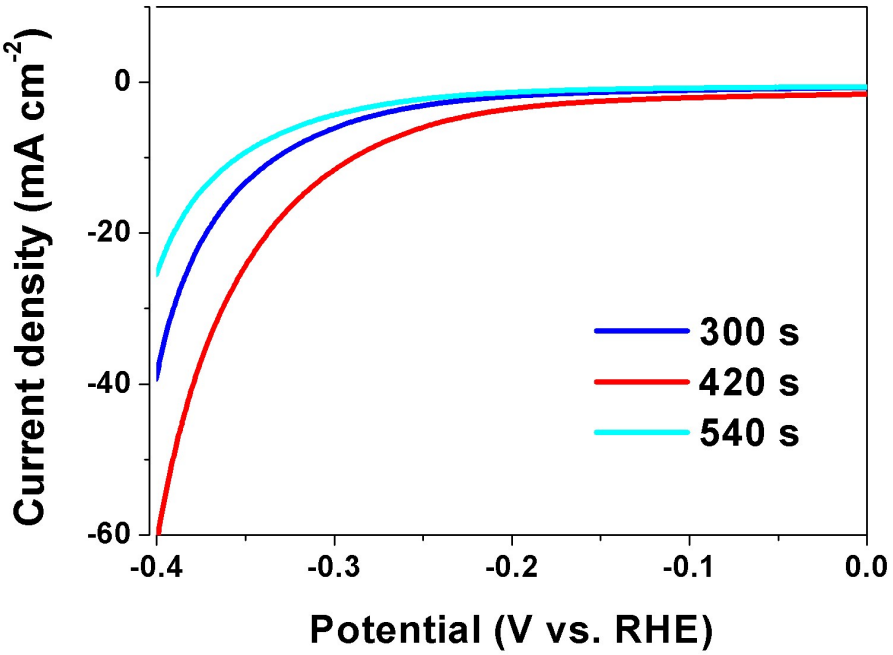

Fig. S5 Polarization curves for $Ni(OH)_2$/CC with different electrodeposition time in 1.0 M KOH with a scan rate of 5 mV s^{-1}

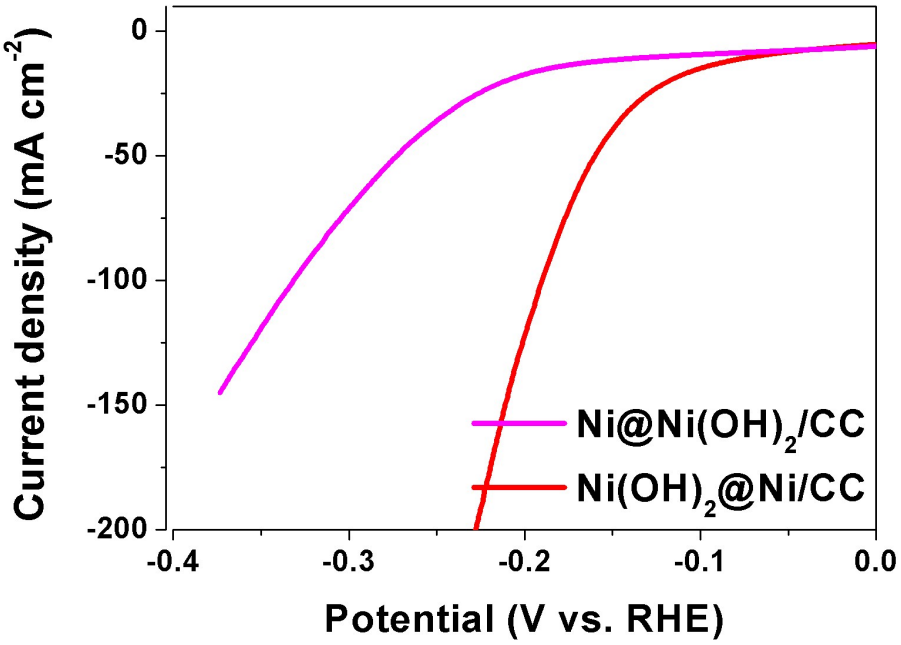

Fig. S6 Polarization curves for $Ni(OH)_2$@Ni/CC and Ni@$Ni(OH)_2$/CC in 1.0 M KOH with a scan rate of 5 mV s^{-1}

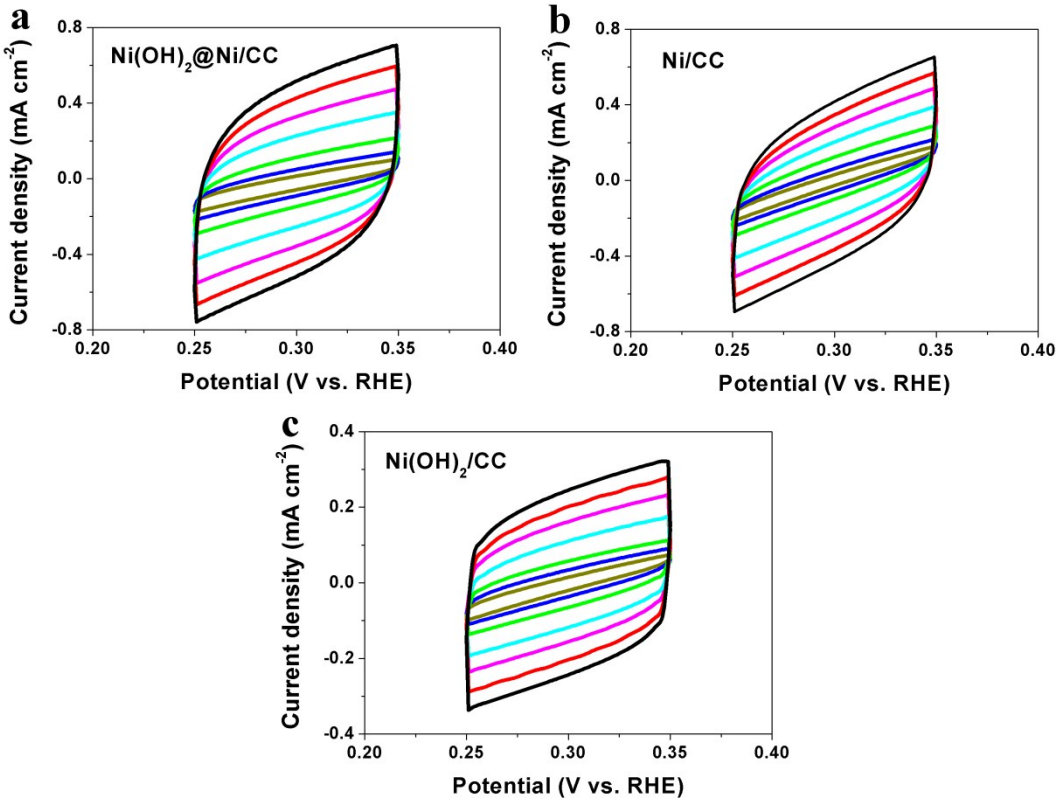

Fig. S7 CVs for (a) $Ni(OH)_2$@Ni/CC, (b) Ni/CC, and (c) $Ni(OH)_2$/CC .

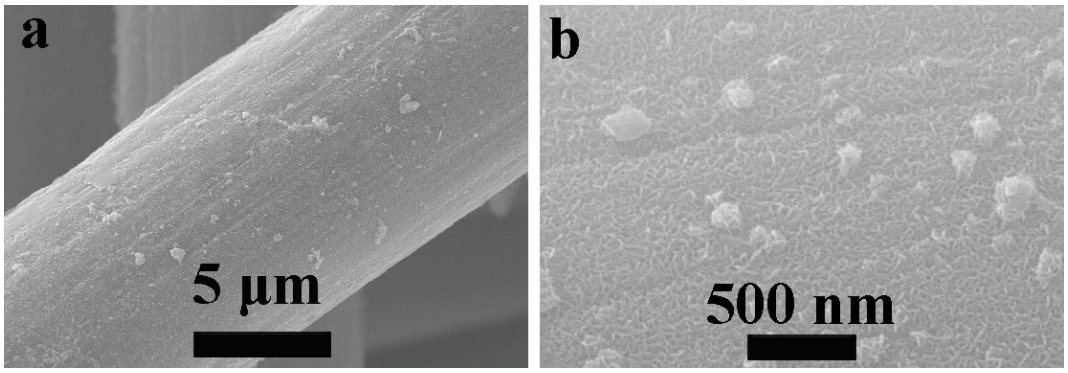

Fig. S8 (a, b) SEM images of $Ni(OH)_2$@Ni/CC after 1000 cycles of continuous cyclic voltammetry.

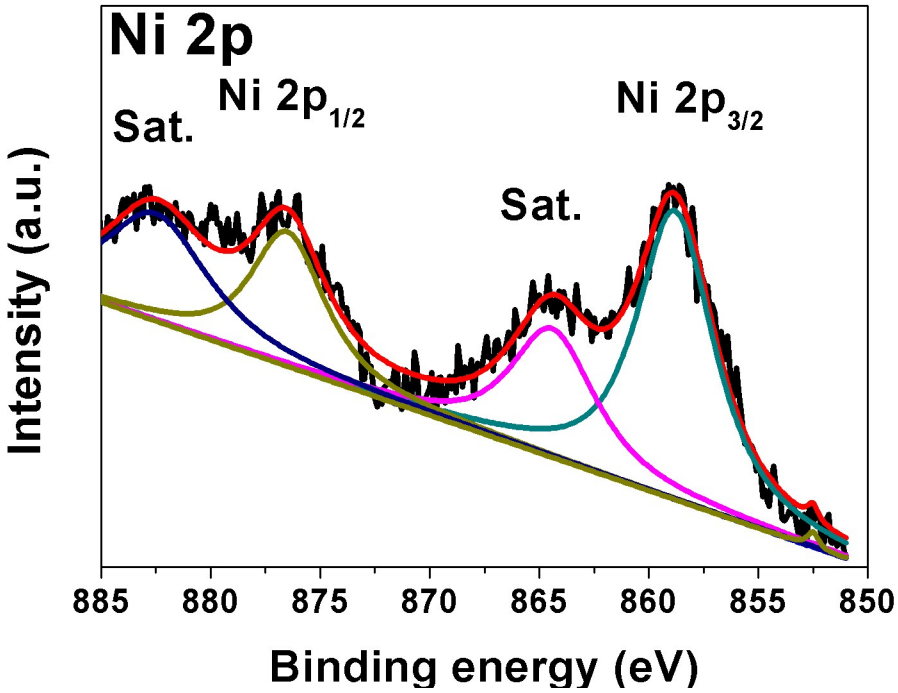

Fig. S9 XPS spectrum in Ni 2p region for $Ni(OH)_2$@Ni /CC after 1000 cycles of catalytic reaction.

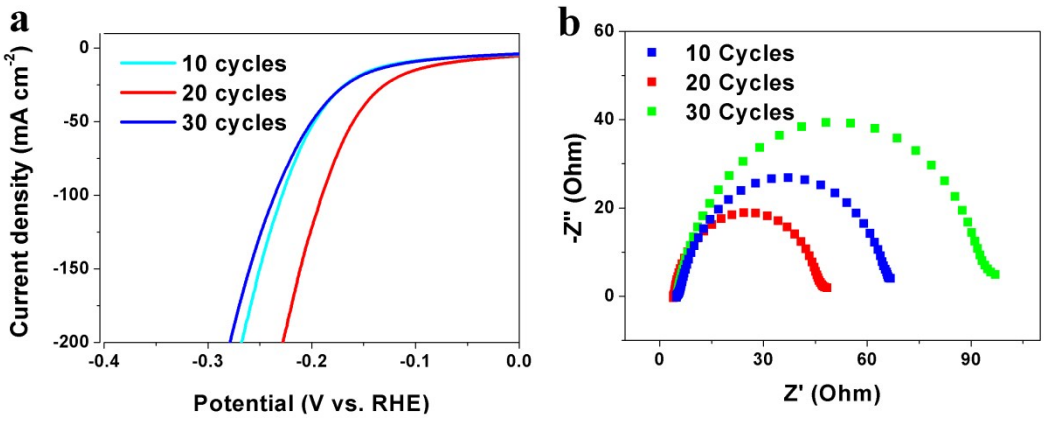

Fig. S10 (a) Polarization curves and (b) Nyquist plots for $Ni(OH)_2$@Ni/CC with electrodeposition of Ni on $Ni(OH)_2$/CC at different duty cycles in 1.0 M KOH with a scan rate of 5 mV s^{-1}.

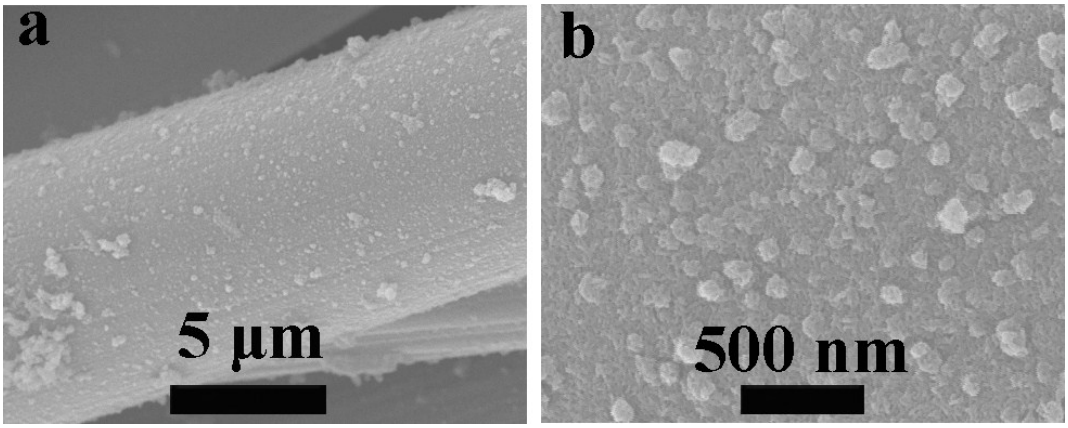

Fig. S11 (a, b) SEM images of $Ni(OH)_2$@Ni/CC after 20 h of bulk water electrolysis in 1 M KOH.

In order to check the validity of Ni electrodeposited on the surface of $Ni(OH)_2$, estimate the layer number of bulk-like slabs Ni is necessary. Four-, five-, and six-layer $Ni(OH)_2$ slabs were examined and the results of corresponding surface energy were showed in table S1 . The calculations of surface energy for $Ni(OH)_2$ slabs converge to a fixed value, 2.01×10^{-3} hartree/Å^2, when it contains more than five layers. Therefore, the slab with five layers is considered to be stable in this paper, which was further used to be the basal for covering Ni atoms. Similarly, the number of Ni layers which covered on $Ni(OH)_2$ slabs were also estimated. Two-, three-, four-, and five-layer Ni cover on $Ni(OH)_2$ slabs were examined (table S2) and the surface energy of Ni layers converges to an approximate fixed value 224.67 hartree/Å^2. The energies will become close because the Ni layer will be reconstructed, as demonstrates in Fig. S10. For taking all possibility into consideration, five-layer Ni covered on the surface of $Ni(OH)_2$ was the optimized condition for our study.

Table S1. The surface energy (γ) of $Ni(OH)_2$ with respect to the number of layers.

Number of layers, N	Surface energy (hartree/Å^2)
4	2.43×10^{-3}
5	2.01×10^{-3}
6	2.01×10^{-3}

Table S2. The surface energy (γ) of $Ni(OH)_2$@Ni with respect to the number of Ni layers.

Number of Ni cover layers, N	Surface energy (hartree/Å^2)
2	244.88
3	244.70
4	244.67
5	244.67

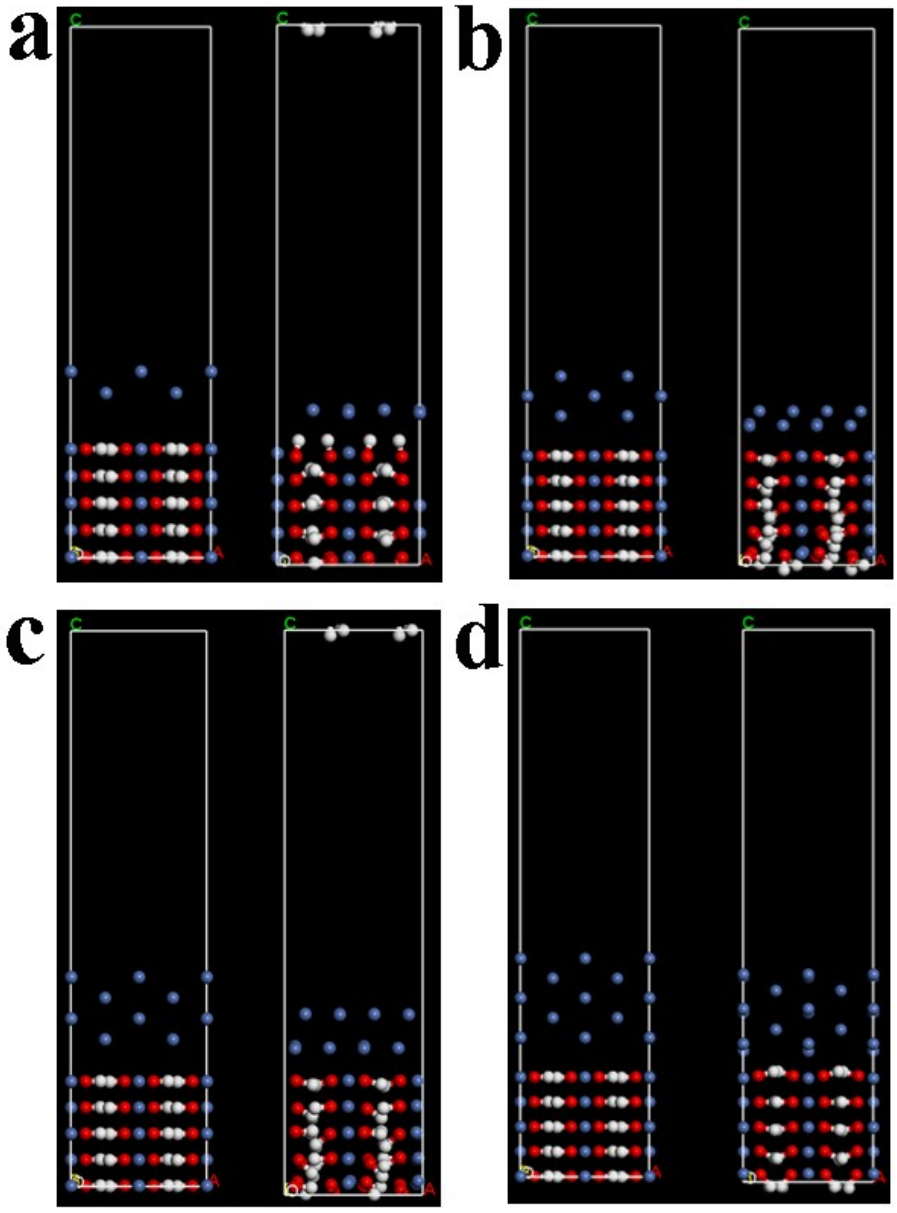
a
b
c
d

Fig. S12 The origin and reconstructed (a) two-, (b) three-, (c) four-, and (d) five-Ni layers covered on the $Ni(OH)_2$.

References

1 B. Delley, *J. Chem. Phys.* 1990, **92**, 508.

2 B. Delley, *J. Chem. Phys.* 2000, **113**, 7756.

3 J. P. Perdew and Y. Wang, *Phys. Rev. B* 1992, **45**, 13244.

4 M. Casas-Cabanas, M. R. Palacin and J. Rodriguez-Carvajal, *Powder Diffr.* 2005, **20**, 334.

5 Y. M. Wang, D. D. Zhao, Y. Q. Zhao, C. L. Xu and H. L. Li, *RSC Adv.* 2012, **2**, 1074.

6 H. J. Monkhorst and J. D. Pack, *Phys. Rev. B* 1976, **13**, 5188.

7 H. Li, C. Tsai, A. L. Koh, L. Cai, A. W. Contryman, A. H. Fragapane, J. Zhao, H. S. Han, H. C. Manoharan, F. Abild-Pedersen, J. K. Norskov and X. Zheng, *Nat. Mater.* 2016, **15**, 48.

8 J. Greeley and J. K. Norskov, *Surf. Sci.* 2007, **601**, 1590.

9 J. K. Norskov, T. Bligaard, A. Logadottir, J. R. Kitchin, J. G. Chen, S. Pandelov and J. K. Norskov, *J. Electrochem. Soc.* 2005, **152**, J23.